

[REDACTED]  
CONSTITUTIVE AND DAMAGE MATERIAL MODELING IN A HIGH  
PRESSURE HYDROGEN ENVIRONMENT

D. A. Russell and L. G. Fritzscheier  
Rocketdyne Division  
Rockwell International  
Canoga Park, California 91303

525-20  
179/14

Numerous components operating in reusable space propulsion systems such as the Space Shuttle Main Engine (SSME) are exposed to high pressure gaseous hydrogen environments. Shown (Figure 1.0) is the SSME Powerhead. Flow areas and passages in the fuel turbopump, fuel and oxidizer preburners, main combustion chamber and injector assembly contain high pressure hydrogen either high in purity or as hydrogen rich steam. As can be seen, this includes many components such as turbine disks and blades, impellers, housings, ducts, etc. Accurate constitutive and damage material models applicable to high pressure hydrogen environments are therefore needed for engine design and analysis. Existing constitutive and cyclic crack initiation models have been evaluated only for conditions of oxidizing environments. The purpose of this effort (Figure 2.0) is to evaluate these models for applicability to high pressure hydrogen environments.

Material behavior is known to be significantly affected by high pressure hydrogen environments (Figure 3.0). For the materials typically employed in rocket engine applications, hydrogen environment embrittlement is most severe near room temperature (Ref. 1). Tensile ductility and notched bar ultimate tensile strength reductions are typically reduced by the hydrogen environment. The room temperature embrittlement effects increase with increasing pressure (Ref. 2). Although the room temperature tensile properties of the superalloys are relatively insensitive to strain rate effects, hydrogen environment embrittlement is strain rate sensitive. Low cycle fatigue lives, especially crack initiation lives, are also reduced by the hydrogen environment (Ref. 3). Thermal activation and time dependent deformation (creep) also become important as temperature increases (Ref. 4). Indications are that the presence of hydrogen can accelerate creep effects by enhancing dislocation mobility (Ref. 5).

The program flow chart (Figure 4.0) is shown for each material. Constitutive modeling effort precedes life modeling. Therefore constitutive test results can be utilized to provide a preliminary projection of crack initiation results, ductility normalized, (Ref. 6) as well as identify target test values for  $\sigma$ ,  $\epsilon$ ,  $\dot{\epsilon}$ , etc. During life testing, specimen constitutive response will be measured to provide an added database for constitutive model verification including any modifications. The experimental phase will begin with the selected isotropic material, followed by the anisotropic material. Both helium and hydrogen testing will be performed to obtain contrasting inert and aggressive environment test results.

Alloy and material model selections as well as test conditions have been defined. Currently, existing data is being surveyed and compiled to provide initial estimates for model constants and to guide test details. Inconel 718 was selected as the isotropic material due to its extensive usage on the SSME, its susceptibility to Hydrogen Environment Embrittlement (HEE) and the existence of service-related hydrogen assisted cracking. PWA 1480 was selected as the single crystal material, due mainly to its development for potential usage on the SSME as a blade material and its known susceptibility to HEE. The nominal properties of

[REDACTED]

these two materials are presented (Figure 5.0) along with the test specimen geometry (Figure 6.0). The maximum test temperatures and pressures (Figure 7.0) correspond to maximum usage on the SSME. Due to the known enhanced HEE effects at room temperature ambient temperature testing shall also be performed.

Recent emphasis on constitutive model development has concentrated on unified viscoplastic models wherein plastic, creep and relaxation strains are treated as one strain component, the inelastic strain. Constitutive model characterization tests (Figure 8.0) will be carried out at both room and elevated temperature in helium and hydrogen environments. The Walker model was chosen for the isotropic material, Inconel 718 and Walker's anisotropic model was selected for PWA 1480 (Figure 9.0, Refs. 7, 8, 9). A modification based on Valanis' material time scale has been developed in-house to extend these rate dependent models into the rate independent (low temperature) regime (Figure 10.0).

Recent crack initiation model development has emphasized life prediction in oxidizing environments under such loading complexities as thermomechanical fatigue, cyclic creep, multiaxial and variable amplitude loading. For assessment in a hydrogen environment, the total strain version of strain range partitioning (TS-SRP) (Refs. 10, 11) was selected for constant amplitude loading conditions. Isothermal testing will be performed to determine the four basic inelastic strain-range life relations, PP, PC, CP, CC as well as the elastic strain-range life relation (Figure 11.0). Due to the preponderance of thermal gradient driven strain cycling of SSME hardware, the most important non-isothermal loop types to consider are out-of-phase PP and PC. To better simulate the impact of thermal mechanical fatigue (TMF), out-of-phase bithermal testing will be performed in PP cycling (Figure 12.0). Reasonable estimates of strain cycle history relative to TMF can be obtained where free thermal expansion strains can be easily subtracted from the total strain.

Cumulative damage will be assessed via the advanced NASA-developed models, Damage Curve Approach (Figure 13.0) and Double Linear Damage Rule (Ref. 12). The nature of these models is to accumulate damage nonlinearly with high-low load sequences being more damaging than low-high. Isothermal tests will be run to provide baseline data and a bithermal LCF test followed by HCF is planned as a verification experiment.

The experimental program as proposed shall include uniaxial monotonic, cyclic (both isothermal and bithermal), creep and relaxation tests to investigate the applicability of these chosen models and to provide a basis for necessary modifications (Figure 14) arising from model deficiencies should they occur.

---

\*Work performed under NASA contract NAS3-26130

## REFERENCES

1. Fritzemeier, L. G.; and Chandler, W. T.: "Hydrogen Embrittlement - Rocket Engine Applications", in Superalloys, Supercomposites and Superceramics, Tien, J. K. and Caulfield, T., Editors, Academic Press Inc., San Diego, 1989.
2. Jewett, R. P.; Walter, R. J.; Chandler, W. T.; and Fromberg, R. P.: "Hydrogen - Environment Embrittlement of Metals", NASA CR-2163, Final Report to NAS8-19(C), 1971.
3. Fritzemeier, L. G.; Walter, R. J.; Meisels, A. P.; and Jewett, R. P.: in "Hydrogen Effects on Material Behavior", Moody, N. R. and Thompson, A. W., Editors, pp. 941-954, 1990.
4. Mucci, J.; and Harns, J. A.: Final Report to NAS8-30744, Exhibits B and C, 1976.
5. Robertson, I. M.; and Birnbaum, H. K.: Acta Met., Vol. 34, No. 3, pp. 353-366, 1986.
6. Halford, G. R.; Saltsman, J. F.; and Hirschberg, M. H.: "Ductility Normalized - Strainrange Partitioning Life Relations for Creep-Fatigue Life Predictions", NASA TM-73737, 1977.
7. Walker, K. P.: "Research and Development for Nonlinear Structural Modeling with Advanced Time-Temperature Dependent Constitutive Relationships", NASA CR-165533, November 1981.
8. Walker, K. P.; and Jordan, E.: "Biaxial Constitutive Modeling and Testing of Single Crystal Superalloy at Elevated Temperature", Engineering Science Software, Inc., Report No. ESS-SCD-8512, September 1985.
9. Chang, K. J.; and Newell, J. F.: "A Material Time Application to Viscoplasticity Theories", in STRUCENG & FEMCAD - Structural Engineering and Optimization, Zarkd, J. and Ohtmer, O., Editors, November, 1990.
10. Saltsman, J. F.; and Halford, G. R.: "Life Prediction of Thermomechanical Fatigue Using Total Strain Version of Strainrange Partitioning (SRP) -- A proposal, NASA TP 2779, February 1988.
11. Manson, S. S.; and Zab, R.: "A Framework for Estimation of Environmental Effect in High Temperature Fatigue", in Proc. of Conf. Environmental Degradation of Engineering Materials, October, 1977.
12. Manson, S. S.; and Halford, G. R.: "Practical Implementation of the Double Linear Damage Rule and Damage Curve Approach for Treating Cumulative Fatigue Damage", NASA TM 81517, April 1980.

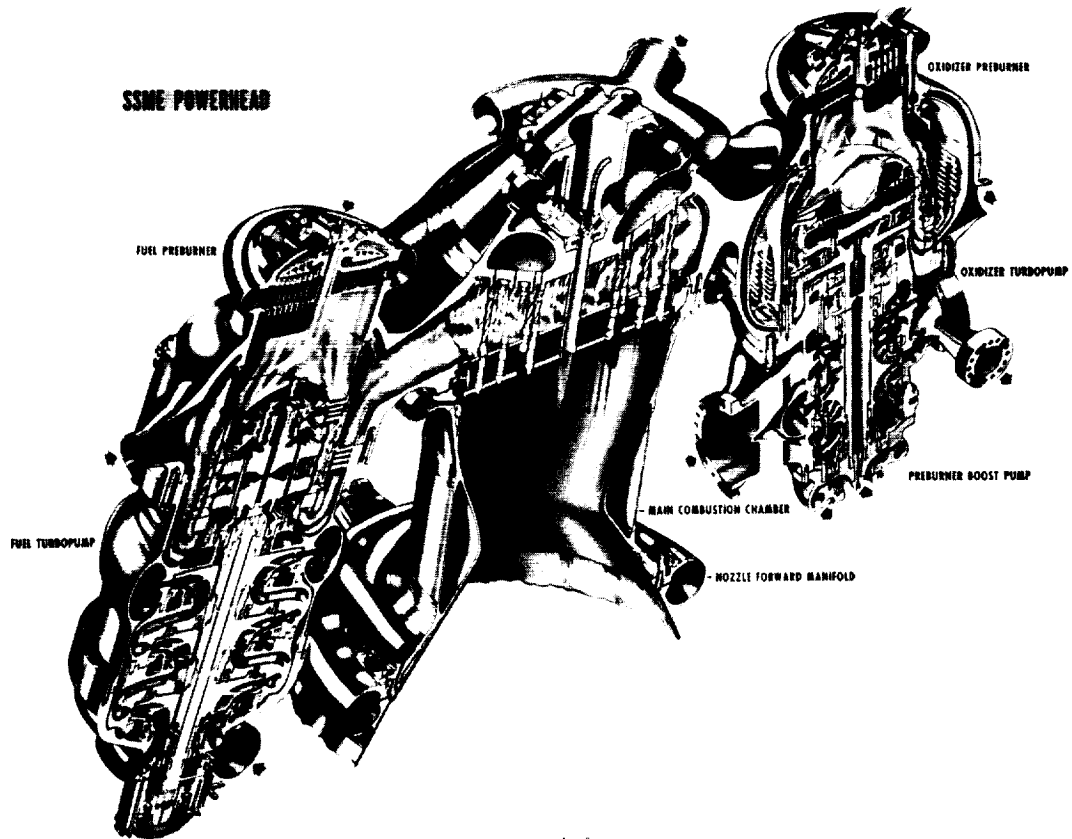
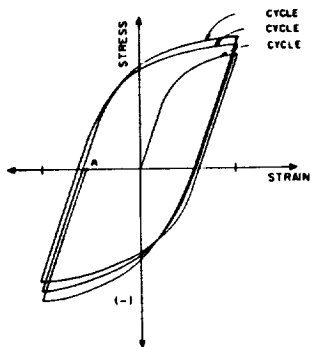


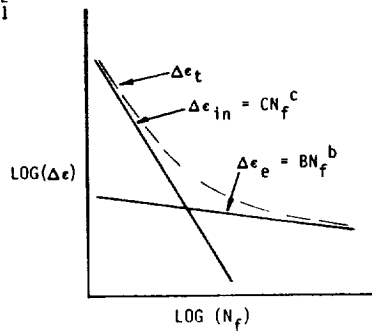
FIGURE 1.0  
COMPONENTS EXPOSED TO HIGH PRESSURE HYDROGEN

- DETERMINE REGIMES OF MATERIAL BEHAVIOR ALTERED BY HIGH PRESSURE H<sub>2</sub>
- EVALUATE EXISTING MATERIAL MODELS FOR HIGH PRESSURE H<sub>2</sub> APPLICABILITY
- PROPOSE MODEL MODIFICATIONS AS REQUIRED

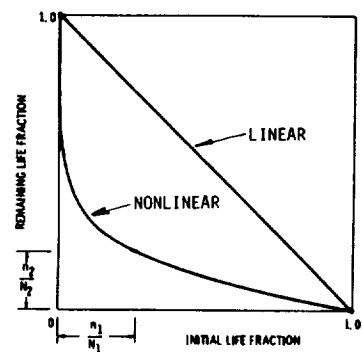
$$\Delta \epsilon_e = B \left( \frac{\Delta \epsilon_{in}}{C} \right)^{b/c}$$



CONSTITUTIVE MODEL



LIFE MODEL



CUMULATIVE DAMAGE MODEL

FIGURE 2.0  
MATERIAL MODELING TASK OBJECTIVES

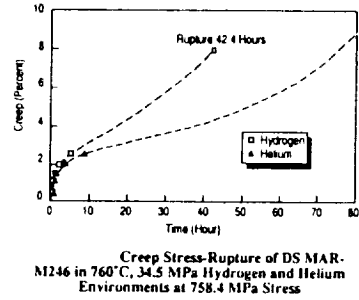
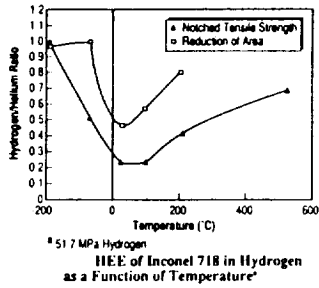
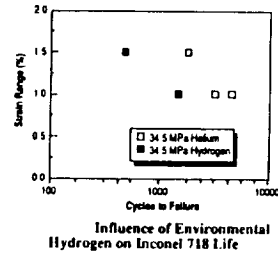
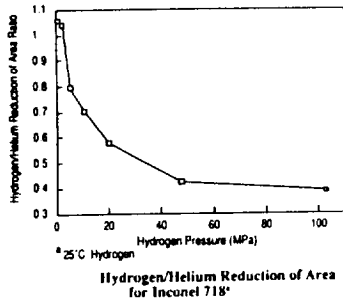


FIGURE 3.0 MATERIAL ISSUES RELATED TO HIGH PRESSURE HYDROGEN

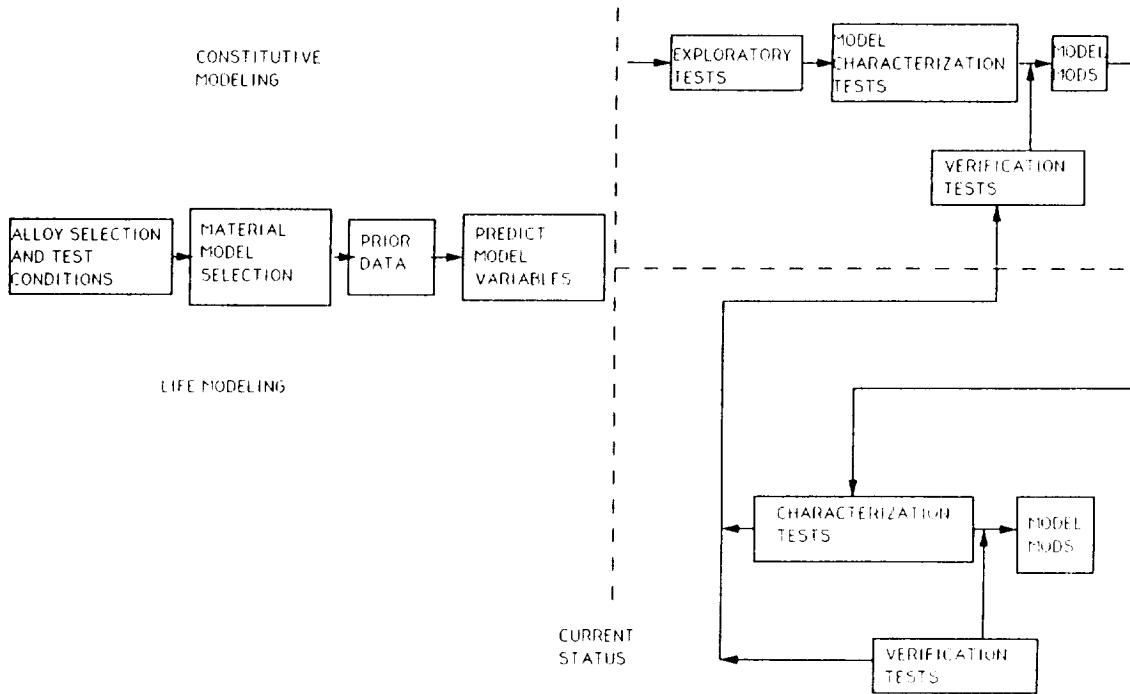


FIGURE 4.0 PROGRAM FLOW (EACH MATERIAL) H2 AND HE TESTING

ISOTROPIC MATERIAL  
INCONEL 718

SINGLE CRYSTAL MATERIAL  
PWA 1480

NOMINAL COMPOSITION (WEIGHT PERCENT)

CR - 19      MO - 3  
NB + T2 - 5    TI - 1.0  
AL - 0.5      FE - 18.5  
NI - BAL.

NOMINAL COMPOSITION (WEIGHT PERCENT)

CR - 10      CO - 5  
W - 4      TI - 1.5  
TA - 12      AL - 5  
NI - BAL.

HEAT TREATMENT

1900°F/30 MIN/AIR COOL  
1400°F/10 HRS/FURNACE COOL TO  
1200°F/HOLD TO 20 HOURS TOTAL

HEAT TREATMENT AND PROCESSING  
(TYPICAL TIMES AND TEMPERATURES)

2350°F/4 HOURS/AIR COOL  
HOT ISOSTATIC PRESS/4 HOURS/2350°F/15 KSI  
1975°F/4 HOURS  
1600°F/32 HOURS

TENSILE PROPERTIES (TYPICAL), KSI

	RT		650°C
	HE	H2	HE
F <sub>TY</sub>	160	160	140
F <sub>TU</sub>	185	185	160
ELONG.%	20	11	20

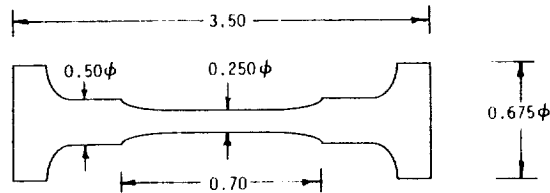
TENSILE PROPERTIES (TYPICAL) <001>, KSI

	RT		870°C
	HE	H2	HE
F <sub>TY</sub>	145	140	100
F <sub>TU</sub>	165	150	140
ELONG.%	5.4	2.5	12

FIGURE 5.0  
MATERIAL SELECTIONS

SPECIMEN DIMENSIONS

HTFV Button Head Fatigue Sample



H<sub>2</sub> VESSEL DESCRIPTION/INSTRUMENTATION DESCRIPTION

- 10,000 PSI/1800°F FATIGUE SYSTEM
- INTERNAL LOAD AND ON-SPECIMEN STRAIN CAPABILITY
- SELF COMPENSATING (TEMP., PRESSURE, ENVIRONMENT) CAPACITANCE EXTENSOMETER
- FULL COMPUTER TEST CONTROL AND DATA MANAGEMENT

FIGURE 6.0  
TEST SPECIMEN AND VESSEL DESCRIPTION

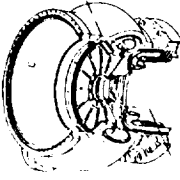
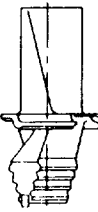
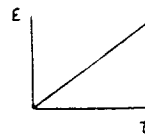
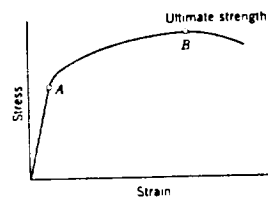
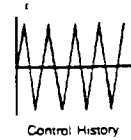
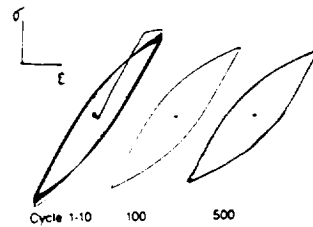
ISOTROPIC MATERIAL - INCONEL 718	SINGLE CRYSTAL MATERIAL - PWA 1480
<ul style="list-style-type: none"> <li>• MAXIMUM USAGE (SSME)</li> <li>• TURBINE HOUSING AND OUTLET MANIFOLD               <ul style="list-style-type: none"> <li>• PRESSURE = 24-34 MPA</li> <li>• HOT GAS TEMP = 650° C</li> </ul> </li> <li>• PUMP INLET TO OUTLET               <ul style="list-style-type: none"> <li>• PRESSURE = 50 MPA</li> <li>• TEMP = 20° C</li> </ul> </li> <li>• MINIMUM TEMP               <ul style="list-style-type: none"> <li>• 20° C</li> </ul> </li> </ul>	<ul style="list-style-type: none"> <li>• MAXIMUM USAGE (SSME)</li> <li>• HIGH PRESSURE TURBOPUMP BLADES               <ul style="list-style-type: none"> <li>• PRESSURE = 34.5 MPA</li> <li>• TEMP = 870° C</li> </ul> </li> <li>• MINIMUM TEMP               <ul style="list-style-type: none"> <li>• 20° C</li> </ul> </li> </ul>
	

FIGURE 7.0  
TEST TEMPERATURES AND PRESSURES

Monotonic Tensile Tests



Cyclic Tests



Creep/Relaxation Tests

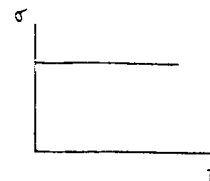
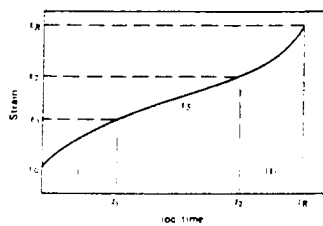


Figure 8.0  
CONSTITUTIVE MODEL CHARACTERIZATION TESTS

## ISOTROPIC CONSTITUTIVE MODEL

**Material Selected:** INCO-718

**Model Selected:** Walker's Isotropic Model

**Modification:** Employ Material Time Concept

**Formulation:**

$$\dot{(\cdot)} = \frac{d}{dz}(\cdot); \quad \text{and} \quad \dot{z} = \frac{dz}{dt}$$

- **The Flow Rule:**

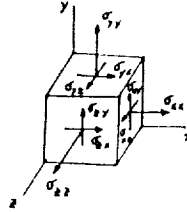
$$\dot{\epsilon}_{ij}^p = \left( \frac{\|\frac{2}{3}\dot{S} - \dot{\Omega}\|}{K} \right)^n \left( \frac{2}{3}\dot{S}_{ij} - \dot{\Omega}_{ij} \right)$$

- **The Evolution Equations:**

$$\begin{aligned} K &= K_1 - K_2 e^{-n_2 R} \\ \dot{\Omega}_{ij} &= (n_1 + n_2) \dot{\epsilon}_{ij}^p + \dot{\epsilon}_{ij}^p \frac{\partial n_1}{\partial \theta} \dot{\theta} \frac{1}{z} \\ &\quad - (n_1 - \dot{\Omega}_{ij} - n_2 \dot{\epsilon}_{ij}^p) \left( \dot{G} - \frac{1}{n_1} \frac{\partial n_1}{\partial \theta} \dot{\theta} \frac{1}{z} \right) \end{aligned}$$

- **The Hooke's Law:**

$$\begin{aligned} \sigma_{ij} &= 2\mu (\dot{\epsilon}_{ij} - \dot{\epsilon}_{ij}^p) + \lambda \delta_{ij} \dot{\epsilon}_{kk} \\ &= 2\mu (\dot{\epsilon}_{ij} - \dot{\epsilon}_{ij}^p \dot{z}) + \lambda \delta_{ij} \dot{\epsilon}_{kk} \end{aligned}$$



## SINGLE CRYSTAL CONSTITUTIVE MODEL

**Material Selected:** PWA-1480

**Model Selected:** Walker's Single Crystal Model

**Modification:** Employ Material Time Concept

**Formulation:**

$$\dot{(\cdot)} = \dot{(\cdot)} \frac{dz}{dt}$$

- **The Flow Rule:** on the  $r^{\text{th}}$  slip system of the 12 octahedral and 6 cubic systems ( $\tau_r$  below is the Schmid shear stress on the slip plane)

$$\dot{\tau}_r = \left( \frac{|\tau_r - \omega_r|}{K_r} \right)^{p-1} \left( \frac{\tau_r - \omega_r}{K_r} \right)$$

- **The Evolution Equations for  $\omega_r$  and  $K_r$**

$$\begin{aligned} \dot{\omega}_r &= \rho_1 \dot{\tau}_r - \rho_2 |\dot{\tau}_r| \omega_r - \rho_3 |\omega_r|^{m-1} \omega_r \\ \dot{K}_r &= \left\{ \sum_{i=1}^{12} [b(q + (1-q)\delta_{ik}) - \eta(K_r - h)] |\dot{\tau}_i| \right\} - h(K_r - K)^p \end{aligned}$$

- **The Inelastic Strain Rate:**

$$\dot{\epsilon}_{ij}^p = \sum_{r=1}^{12} a_r \dot{\tau}_r + \sum_{r=1}^6 b_r \dot{\tau}_r$$

- **The Hooke's Law:**

$$\sigma_{ij} = D_{ijkl} \left\{ \dot{\epsilon}_{kl} - \sum_{r=1}^{12} (\epsilon_{kl}^p)^r + \sum_{r=1}^6 (\epsilon_{kl}^p)^{r+h} \right\}$$

Figure 9.0 WALKER'S UNIFIED CONSTITUTIVE MODELS

## Basic Ideal

- Material experiences deformation and remembers its deformation history.
- Thus, the time felt by material should also include the effect of deformation.

## Expression of the Material Time Increment

$$dz = \sqrt{\lambda_{ijkl} \epsilon_{ij} \epsilon_{kl} + g dt^2}$$

where  $\lambda_{ijkl}$  and  $g$  are material parameters.

## Proposed Use of the Material Time

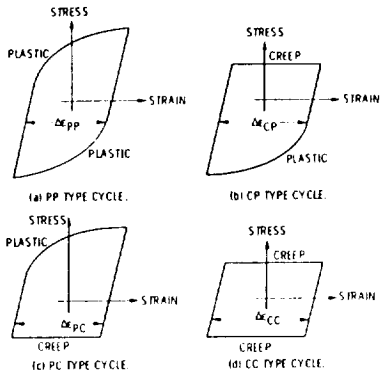
Change the time derivatives in a viscoplastic formulation into derivatives with respect to the material time.

- \* It reduces to the original viscoplastic formulation when  $\lambda_{ijkl}$  is null and  $g = 1$  (used for high temperature cases)
- \* It has no rate dependence while plasticity remains when  $\lambda_{ijkl}$  is constant and  $g = 0$  (applicable for low temperatures)

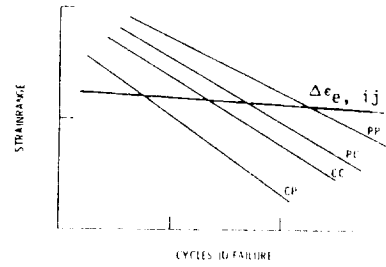
Figure 10.0 THE MATERIAL TIME CONCEPT

INELASTIC SRP CYCLE  
TYPES/IDEALIZED LOOPS

( $R_e = -1.0$ )



TYPICAL PARTITIONED STRAIN  
RANGE-LIFE RELATIONS



INTERACTION DAMAGE RULE:

$$\sum \frac{F_{ij}}{N_{ij}} = \frac{1}{N_{fo}}, \quad ij = pp, pc, cp, cc$$

FIGURE 11.0  
DAMAGE MODEL TS-SRP (ISOTHERMAL)  
 $R_e = -1.0$  AND  $R_e = 0.0$  (PP)

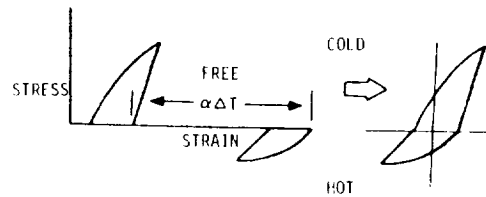
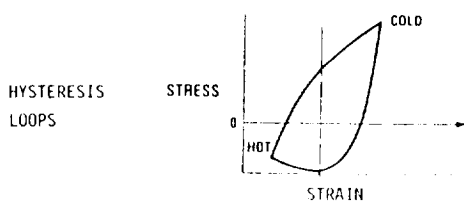
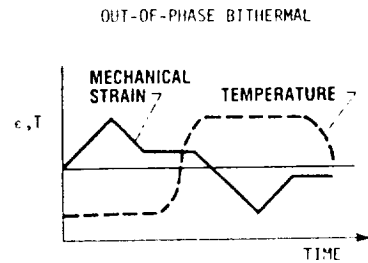
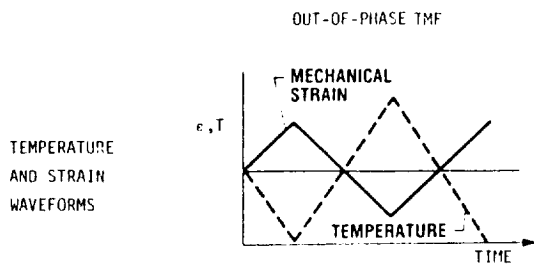
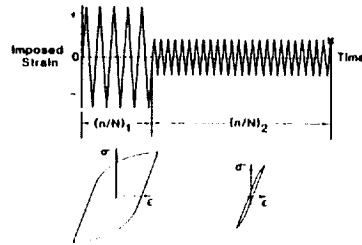


FIGURE 12.0  
COMPARISON BETWEEN BITHERMAL AND TMF CYCLING

TWO STEP LOADING PATTERN



TWO LEVELS OF LOADING

$N_1$  &  $N_2$

$$\frac{n_2}{N_2} = 1 - \left[ \frac{n_1}{N_1} \right] \left[ \frac{N_1}{N_2} \right]^\alpha$$

← REMAINING LIFE FRACTION

← INITIAL LIFE FRACTION

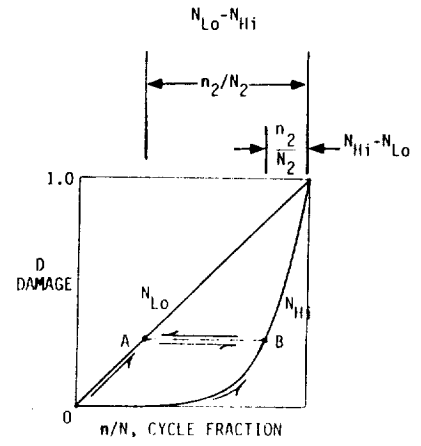


FIGURE 13.0  
DAMAGE CURVE APPROACH